State Damping Control: A Novel Simple Method of Rotor UAV with High Performance

Run Ye[1], Peng Liu[1], Kaibo Shi[2], and Bin Yan[1].

[1]School of Automation Engineering, University of Electronic Science and Technology of China, Chengdu, 611731 China
[2]School of Electronic Information and Electrical Engineering, Chengdu University, Chengdu, 611731 China

Corresponding author: Run Ye (e-mail: rye@uestc.edu.cn).

ABSTRACT Sliding Mode Control and Adaptive Control are widely studied in the area of Rotor UAV in recent years. Although the performance of Rotor UAV with these controllers show high command tracking ability and good robustness, they are limited by model accuracy so that they cannot take place PID. In this paper, a novel method named State damping control is proposed to be a candidate for the traditional PID method. Our proposed State Damping Control is inspired by the format of air resistance. The method is based on the general idea that resistance will make a system easy to stabilize. State damping control is independent of model accuracy and just uses three parameters to control attitude, so it is easy to realize. Krasovskii Theorem is used to give the evidence that State damping control is asymptotic stable in our considered state space. Finally, simulations are implemented in C++ on VS2017, it demonstrates that State damping control is easy to be tuned and robust to wind attack and inertial parameters. Compared with PID, our proposed method is robust to wind disturbances obviously.

INDEX TERMS State damping control, robust control, nonlinear systems, computational methods

I. INTRODUCTION

UAV gradually becomes a hot word with the development of microcontrollers and miniaturization of sensors. The technology to manufacture UAV is a way that a country to show military strength. Besides, civilian UAVs become a pattern for people to take photos or do dangerous missions. Recently, many papers focus on Environmental Monitoring assisted by UAV photos, as in [1-3]. Rotor UAV (RUAV) is more widely used in the civilian market than fixed-wing UAV due to advantages including friendly operation and good performance of hovering, as described in [4-5]. PID controller is described in [6-9] which is the most successful and practical controller for RUAV to easy design and model independence.

As the thrust of RUAV is limited, the weight of the onboard microcontroller is also limited so that the calculation ability of the onboard microcontroller is often very low. The dynamics of RUAV are nonlinear, strong coupling, and multivariate, so it is hard to control RUAV with the high performance of command tracking and robustness in a complex natural environment. The algorithm design of RUAV is dedicated not only to improve the control precision and robustness but also try to make the calculation simple. PID controller is simple and can satisfy

the normal application of RUAV. However, traditional PID controller performance will degrade with parametric changes or environmental disturbance. Numerous studies are carried out to improve control precision and robustness. However, fewer of them intended to make the calculation simple so that the algorithm is more applicable for embedded processors.

The backstepping method changes a complex system into many simple subsystems by decomposing RUAV into position subsystem, velocity subsystem, and attitude subsystem. Thus, cascaded Lyapunov functions are often used to deduce control law. In [39], a standard backstepping procedure is derived to control a RUAV. The key point of this method is to linearize the RUAV system by compensating nonlinear dynamics, which means that model of RUAV is needed. As a synthesis work in [38], a parameter scheduled backstepping method is proposed and experiments show the effectiveness of their method. Compared with PID, the backstepping method has a more strict theory analysis to keep the system stable. Actually, the analysis is based on model accuracy. In cascaded controllers as backstepping, there are many parameters to be tuned. If one sub-controller is tuned badly, the other sub-controller will work in a saturation state.

The robustness of Sliding Mode Control (SMC) is augmented in many papers, and SMC shows superb control precision along with RUAV nonlinear dynamics [10-13, 34, 35]. Additionally, SMC also has the ability to accommodate inner or external uncertainties. Higher-order SMC is proposed to control systems and the robustness can be ensured by theory [14-15]. However, if this method is used to control RUAV, there are two difficulties. The one is this method has to know the accurate mathematic model of RUAV which is hard to obtain, the other is the complicity to get the control law for numerous matrixes, fractional power, and derivatives calculations. In [16], quasi-continuous SMC is used to control a real quadrotor in the presence of whole aerodynamics and electrodynamics. The controller in [16] is robust, but the process to obtain full aerodynamic coefficients is rather difficult. The authors in [16] spend almost four years to obtain aerodynamic coefficients and their parameters cannot be used to another RUAV. In [38], the SMC controller is compared with the PID and Backstepping method. Their experimental results show that PID, SMC, and Backstepping methods have little difference in trajectory tracking. This shows that a model-based controller as SMC is limited by model accuracy in actual use.

Model reference adaptive control (MRAC) is to use the state errors or output errors between the reference model and real system to obtain parameter adjustment signal or auxiliary control signal so that the system can accommodate the inner or external uncertainties [17-20, 36, 37]. If MRAC is used to design the RUAV, it is possible to improve the robustness, especially in system failures—blade-broken and actuator failures. In [21], the MIT rule is promised to provide robustness in height control, but the stability of the system cannot be guaranteed. Another limitation of the MIT rule is this method is hard to design a multi-input multi-output system and RUAV is that kind of system. In [22], the Lyapunov function is proposed to guarantee the robustness in height and attitude control, experiments show the effectiveness of the controller. There are also two limitations in this work: firstly, the application situation is just a small angle; secondly, there is a ground computer to assist computation, so it is hard for remote flight. In [23], an omnibus controller which is a combination of SMC, FLC, and Radial Base Function Neural Network (RBFNN) is designed; the performance of robustness and control precision is perfect showed by the simulation. Similarly, the limitation is due to the complexity of identify model parameters.

As described above, the stable analysis of backstepping, SMC, MRAC is limited by the accuracy of the dynamics model. As we know, aerodynamics and electrodynamics are difficult to identify for civil RUAV. Therefore, these approaches cannot take place PID to achieve better performance.

The main contribution of this paper is that a novel control method named State Damping Control (SDC) is proposed. Our proposed method is independent of the model, which means the proposed method will not be limited by model accuracy. Furthermore, our method is as simple as PID and more robust than PID.

The details of our contributions are as follows.

• Inspired by the air-resistance model, robust SDC which is simple to design and easy to obtain control parameters is proposed.

• Using stability proof and positive definite matrix discriminative approach to estimate gains that can guarantee system globally asymptotically stable.

• Simulations are implemented in C++ and the results show the effectiveness of SDC to control the RUAV attitude system.

This paper is organized as follows. Section II describes how to establish the RUAV mathematic model and it is linearized for simulation convenience. Section III elaborates on the process to propose SDC and shows a method to select gains based on *Krasovskii Theorem* and positive definite matrix discriminative approach. Section IV describes a key algorithm for C++ simulation, an example is given to show the details to select parameters and the effectiveness of SDC. Section V summarizes the results and give some conclusions.

II. Mathematical Model

This paper takes the RUAV as an approximate symmetry rigid body so that the off-diagonal terms of inertia matrix J can be taken as small numbers. In the process of establishing the mathematic model of RUAV, the force is considered as resultants force which including thrust, gravity, and air-resistance, etc. For this purpose, we use modern control theory to analyze the stabilization of RUAV, and the non-linear derivative equations are described in the state-space. Furthermore, it is linearized based on the Taylor series for simulation convenience.

A. Coordinate system

There are three coordinate frames involved in this paper: geocentric inertial frame, navigational coordinate frame, and body coordinate frame.

A geocentric inertial frame is defined as: the original location coincides with the earth centroid and x-direction directs from earth centroid toward the vernal equinoctial point, z-direction directs from earth centroid toward protocol geographic North Pole. The right-hand helix relationship is satisfied among the three axes.

The navigational coordinate frame is defined as: the original location coincides with the body centroid, x-direction towards the east, y-direction towards the north, and z-direction towards vertical upward.

The body coordinate frame is defined as: the original location coincides with the body centroid, y-direction towards heading, x-direction towards the right direction of heading. These three axes satisfy the right-hand helix relationship.
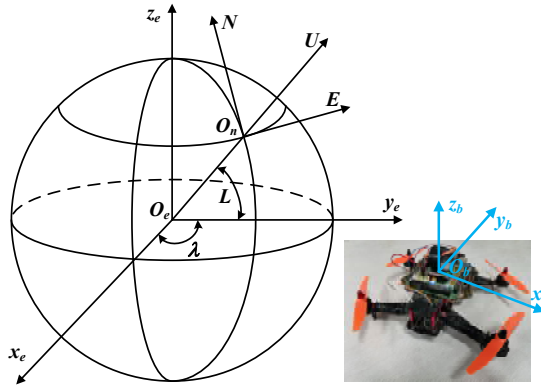
The three coordinate frames can be seen in Fig. 1.

Figure 1. Coordinate frames including geocentric inertial frame, navigational coordinate frame and body coordinate frame .

The translations between the body coordinate frame and navigation coordinate frame are generally used in RUAV attitude calculation. In general, a rotation matrix is used for the translation. There are two common methods to describe RUAV altitude, Euler angles, and quaternion [24-25,33]. It is assumed that pitch and roll are both less than 90° such that Euler angles are totally suitable in this paper [16-17]. Euler angles have clear physical signs that can be easily understood. Furthermore, the roll, pitch, and yaw inputs can be seen as independent of hovering assumptions.

The fundamental of Euler angle is that any Cartesian coordinate frame can coincide with another Cartesian coordinate frame through three rotations. For clear physical significance, the rotation order is as first Yaw (Y), then Pitch (P), and last Roll (R). The rotation relationship is shown in (1) and is an orthogonal matrix.

Define

$$sP = \sin P, \quad cP = \cos P, \quad sR = \sin R$$
$$cR = \cos R, \quad sY = \sin Y, \quad cY = \cos Y$$

The rotation matrix can be written as $x_b = C_n^b x_n$

$$C_n^b = \begin{bmatrix} cPcY - sPsRsY & cRsY + sPsRcY & -cPsR \\ -cPsY & cPcY & sP \\ sRcY + sPcRsY & sRsY - sPcRcY & cPcR \end{bmatrix}. \quad (1)$$

The three Euler angles of RUAV are determined by initial conditions and angular velocity ω which is measured by gyroscope integrated into the MPU6050. Assuming the effects of earth rotation can be neglected, in other words, the angular velocity measured by gyroscope can be seen as the relative angular velocity between navigation coordinate frame and body coordinate frame [6]. Thus, the relationship between Euler angles and angular velocity ω is shown in (2).

$$\begin{bmatrix} \dot{P} \\ \dot{R} \\ \dot{Y} \end{bmatrix} = \frac{1}{\cos P} \begin{bmatrix} \cos P \cos R & 0 & \sin R \cos P \\ \sin P \sin R & \cos P & -\cos R \sin P \\ -\sin R & 0 & \cos R \end{bmatrix} \begin{bmatrix} \omega_x \\ \omega_y \\ \omega_z \end{bmatrix} \quad (2)$$

where ω_x, ω_y, and ω_z are the projections of angular velocity ω in the body coordinate frame.

B. Mathematics Model

The motion of the rigid-body can be divided into translational dynamics and attitude dynamics. In this paper, Newton-Euler equations[40] are used to describe rigid-body dynamics, which is shown in state space as

$$\begin{cases} \dot{v} = v \times \omega + F / m \\ \dot{\omega} = -J^{-1} (\omega \times J\omega) + J^{-1} M \end{cases} \quad (3)$$

The matrix J is described in the body coordinate frame so that J is constant.

$$J = \begin{bmatrix} J_x & J_{xy} & J_{xz} \\ J_{xy} & J_y & J_{yz} \\ J_{xz} & J_{yz} & J_z \end{bmatrix} \quad (4)$$

It is assumed that the off-diagonal terms of the inertia matrix J can be taken as a small number, when there are two small numbers multiply it is possible to be neglected. Note that this assumption is more carefully consider the asymmetry of a mass of RUAV than common models [26-28].

We expand (3)

$$\begin{cases} \dot{v}_x = v_y \omega_z - v_z \omega_y + F_x / m \\ \dot{v}_y = -v_x \omega_z + v_z \omega_x + F_y / m \\ \dot{v}_z = v_x \omega_y - v_y \omega_x + F_z / m \\ \dot{\omega}_x = c_1 \omega_x \omega_y + c_2 \omega_x \omega_z + c_3 \omega_y \omega_z + c_4 (\omega_z^2 - \omega_y^2) + M_1 \\ \dot{\omega}_y = c_5 \omega_x \omega_y + c_6 \omega_x \omega_z + c_7 \omega_y \omega_z + c_8 (\omega_x^2 - \omega_z^2) + M_2 \\ \dot{\omega}_z = c_9 \omega_x \omega_y + c_{10} \omega_x \omega_z + c_{11} \omega_y \omega_z + c_{12} (\omega_y^2 - \omega_x^2) + M_3 \end{cases} \quad (5)$$

where

$$c_1 = \frac{J_{xz}(J_x - J_y + J_z)}{J_x J_z} \quad c_2 = \frac{J_{xy}(-J_x - J_y + J_z)}{J_x J_y}$$

$$c_3 = \frac{J_y - J_z}{J_x} \quad c_4 = -\frac{J_{yz}}{J_x}$$

$$c_5 = \frac{J_{yz}(J_x - J_y - J_z)}{J_y J_z} \quad c_6 = \frac{-J_x + J_z}{J_y}$$

$$c_7 = \frac{J_{xy}(J_x + J_y - J_z)}{J_x J_y} \quad c_8 = -\frac{J_{xz}}{J_y}$$

$$c_9 = \frac{J_x - J_y}{J_z} \quad c_{10} = \frac{J_{yz}(-J_x + J_y + J_z)}{J_y J_z}$$

$$c_{11} = \frac{J_{xz}(-J_x + J_y - J_z)}{J_x J_z} \quad c_{12} = -\frac{J_{xy}}{J_z}$$

$$M_1 = \frac{1}{J_x} M_x + \frac{J_{xy}}{J_x J_y} M_y + \frac{J_{xz}}{J_x J_z} M_z$$

$$M_2 = \frac{J_{xy}}{J_x J_y} M_x + \frac{1}{J_y} M_y + \frac{J_{yz}}{J_y J_z} M_z$$

$$M_3 = \frac{J_{xz}}{J_x J_z} M_x + \frac{J_{yz}}{J_y J_z} M_y + \frac{1}{J_z} M_z$$

where F_x, F_y, F_z, M_x, M_y, and M_z are the projections of resultant forces of RUAV in body coordinate frame; v_x, v_y,

v_z, ω_x, ω_y, and ω_z are the selected state variables, represent the RUAV velocity and angular velocity described in body coordinate frame. Equation 5 is the established RUAV mathematics model in this paper.

C. Linear dispose

Equation (5) is a group of non-linear differential equations, it is hard to use in the simulation due to the non-linear character. Therefore, we use the Taylor series to expand (5) at the point $(v_{x0}, v_{y0}, v_{z0}, \omega_{x0}, \omega_{y0}, \omega_{z0})$ and it can be written as (6).

$$\dot{x} = Ax + Bu \tag{6}$$

where

$$A = \begin{bmatrix} 0 & \omega_{z0} & -\omega_{y0} & 0 & -v_{z0} & v_{y0} \\ -\omega_{z0} & 0 & \omega_{x0} & v_{z0} & 0 & v_{x0} \\ \omega_{y0} & -\omega_{x0} & 0 & -v_{y0} & -v_{x0} & 0 \\ 0 & 0 & 0 & a_{44} & a_{45} & a_{46} \\ 0 & 0 & 0 & a_{54} & a_{55} & a_{56} \\ 0 & 0 & 0 & a_{64} & a_{65} & a_{66} \end{bmatrix} \tag{7}$$

and

$$a_{44} = c_1 \omega_{y0} + c_2 \omega_{z0}$$
$$a_{45} = c_1 \omega_{x0} + c_3 \omega_{z0} - 2c_4 \omega_{y0}$$
$$a_{46} = c_2 \omega_{x0} + c_3 \omega_{y0} + 2c_4 \omega_{z0}$$
$$a_{54} = c_5 \omega_{y0} + c_6 \omega_{z0} + 2c_8 \omega_{x0}$$
$$a_{55} = c_5 \omega_{x0} + c_7 \omega_{z0}$$
$$a_{56} = c_6 \omega_{x0} + c_7 \omega_{y0} - 2c_8 \omega_{z0}$$
$$a_{64} = c_9 \omega_{y0} + c_{10} \omega_{z0} - 2c_{12} \omega_{x0}$$
$$a_{65} = c_9 \omega_{x0} + c_{11} \omega_{z0} + 2c_{12} \omega_{y0}$$
$$a_{66} = c_{10} \omega_{x0} + c_{11} \omega_{y0}$$

Select $u=[F_x/m \; F_y/m \; F_z/m \; M_x \; M_y \; M_z]^T$, we can obtain

$$B = \begin{bmatrix} 1 & 0 & 0 & 0 & 0 & 0 \\ 0 & 1 & 0 & 0 & 0 & 0 \\ 0 & 0 & 1 & 0 & 0 & 0 \\ 0 & 0 & 0 & 1/J_x & J_{xy}/(J_x J_y) & J_{xz}/(J_x J_z) \\ 0 & 0 & 0 & J_{xy}/(J_x J_y) & 1/J_y & J_{yz}/(J_y J_z) \\ 0 & 0 & 0 & J_{xz}/(J_x J_z) & J_{yz}/(J_y J_z) & 1/J_z \end{bmatrix} \tag{8}$$

Note that the point $(v_{x0}, v_{y0}, v_{z0}, \omega_{x0}, \omega_{y0}, \omega_{z0})$ can change with time when used in the simulation or reference model. Therefore, the non-linear differential equations expressed in (5) expand to linear differential equations expressed in (6). It is easy to realize (6) on a computer.

III. STATE DAMPING CONTROL

Euler angles can be calculated by (2) whose results are determined by angular velocity and we can see the strong coupling in angular velocity from (5). Therefore, Euler angles have a strong coupling so that it is difficult to realize high tracking precision and globally asymptotically stable.

Furthermore, heading and velocity are determined by Euler angles. It is obvious that attitude control is the most important part of the RUAV flight. In this paper, we just consider attitude control which includes the dominant dynamics.

A. Problem Formulation

The open-loop attitude system is expressed in (9) and (10). As the input of equation (10) is determined by equation (9), the stability of the whole system is determined by equation (9).

State equations

$$\begin{cases} \dot{\omega}_x = c_1 \omega_x \omega_y + c_2 \omega_x \omega_z + c_3 \omega_y \omega_z + c_4 \left(\omega_z^2 - \omega_y^2 \right) + M_1 \\ \dot{\omega}_y = c_5 \omega_x \omega_y + c_6 \omega_x \omega_z + c_7 \omega_y \omega_z + c_8 \left(\omega_x^2 - \omega_z^2 \right) + M_2 \\ \dot{\omega}_z = c_9 \omega_x \omega_y + c_{10} \omega_x \omega_z + c_{11} \omega_y \omega_z + c_{12} \left(\omega_y^2 - \omega_x^2 \right) + M_3 \end{cases} \tag{9}$$

$$\begin{bmatrix} \dot{P} \\ \dot{R} \\ \dot{Y} \end{bmatrix} = \frac{1}{\cos P} \begin{bmatrix} \cos P \cos R & 0 & \sin R \cos P \\ \sin P \sin R & \cos P & -\cos R \sin P \\ -\sin R & 0 & \cos R \end{bmatrix} \begin{bmatrix} \omega_x \\ \omega_y \\ \omega_z \end{bmatrix} \tag{10}$$

The work requires to do is to design the control law for the former system so that the system can output expected angles. The essential description is how to design M_x, M_y, and M_z according to the information that can be obtained.

B. Proposed SDC

In preliminary work, we tried to use the PID controller to stabilize the attitude system and a simulation was done. However, we failed to stabilize the system as the sequence of neglecting the air-resistance. Based on this phenomenon, we suppose 'the existence of air-resistance contributes to stabilizing the attitude system'. If a fictitious air-resistance is added to the attitude system, it may provide stabilization to the system. The follows will introduce how it works.

The foundation of the control law is an air-resistance model. To obtain the air-resistance mathematic model, a simple physical model is used to estimate it, as shown in Fig. 2. A plank rotates fixed-axis with angular speed ω, the length of the plank is R and the height is l. There will be a force F_f on the forward surface of the plank derived from the reacting of wind. There will be another force F_b on the back surface of the plank derived from the air adsorption.
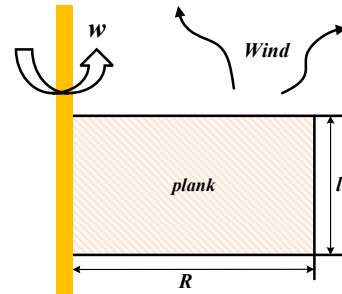

Figure 2. Physical model to estimate air-resistance.

F_b can be seen as a static friction, which can be written as $F_b = C_2 sign(\omega)$

where C_2 is a positive constant and

$$sign(\omega) = \begin{cases} -1 & \omega < 0 \\ 1 & \omega > 0 \end{cases}$$

Suppose the air density is ρ, follow the rule given by (4), F_f is estimated as

$$\left| F_f \right| dt = \rho \frac{\omega dt R^2 l}{2} \cdot \frac{\omega R}{2} = C_1 \omega^2 \qquad (11)$$

where C_1 is a positive constant. Thus, we can obtain the total air-resistance F_a.

$$F_a = F_b + F_f = C_1 \omega^2 sign(\omega) + C_2 sign(\omega) \qquad (12)$$

The second part of (12) $C_2 sign(\omega)$ does not exist in [16]. This means that the second part is insignificant and can be neglected in actual air-resistance estimation. However, the second part is important in the control law and the reason will be given subsequently. Since we care more about moments when the RUAV is desired to output expected angles, rewrite (12) as

$$\begin{aligned} M_a &= F_a \frac{R}{2} = C_1 \frac{R}{2} \omega^2 sign(\omega) + C_2 \frac{R}{2} sign(\omega) \\ &= Z_1 \omega^2 sign(\omega) + Z_2 sign(\omega). \end{aligned} \qquad (13)$$

For the purpose of showing fictitious air-resistance is different from the actual air-resistance, we estimate the actual air-resistance below, and the fictitious air-resistance is described in section IV. From the comparison with the article [16], we know that Z_2 is very small when this model is used to describe actual air-resistance. The estimation of Z_1 associated with actual air-resistance is as follows.

$$R = l = 0.45\text{m}, \rho = 1.2\text{kg}/\text{m}^3$$

The size is similar to a RUAV in our lab. The value of Z_1 can be estimated as

$$Z_1 = \frac{\rho R^4 l}{8} = 2.7 \times 10^{-3} \text{kg} \cdot \text{m}^2 \qquad (14)$$

We will compare actual air-resistance with fictitious air-resistance in section IV. Equation (14) is the air-resistance model we used to design control law for the system combined by (9) and (10). Note that we just use the form of air-resistance model, as the specific value of the air-resistance coefficient depends on the system stabilization requirement. Thus, we introduce the control law as (15) and the gains z_1 and z_2 need to be adjusted by simulations or experiments.

$$u_s = \begin{bmatrix} M_x \\ M_y \\ M_z \end{bmatrix} = -z_1 \begin{bmatrix} \omega_x^2 sign(\omega_x) \\ \omega_y^2 sign(\omega_y) \\ \omega_z^2 sign(\omega_z) \end{bmatrix} - z_2 \begin{bmatrix} sign(\omega_x) \\ sign(\omega_y) \\ sign(\omega_z) \end{bmatrix} \qquad (15)$$

Now it is time to explain why the second part in (12) is significant. Since the second part in (15) is derived from (12), the question becomes why the second part in u_s is significant. For the attitude system when the output angles are around the expected angles, the angular velocity ω is near zero so that the first part of u_s is near zero too. If u_s doesn't have the second part, there will take a very long time to vibrate around the expected angles. If u_s has the

second part, even the angular velocity ω is near zero, the value of u_s will tend to be constant so that the attitude system can quickly stabilize at the expected angles. Therefore, the second part of u_s is significant.

There are several *sign* functions in u_s, the controller will chatter when the system near the expected angles, which is because the *sign* will switch regularly. This problem also exists in SMC, and many researchers proposed practical approaches to deal with it [29-30]. This paper refers to the work in [31] using a smooth function to replace the initial function, see as (16).
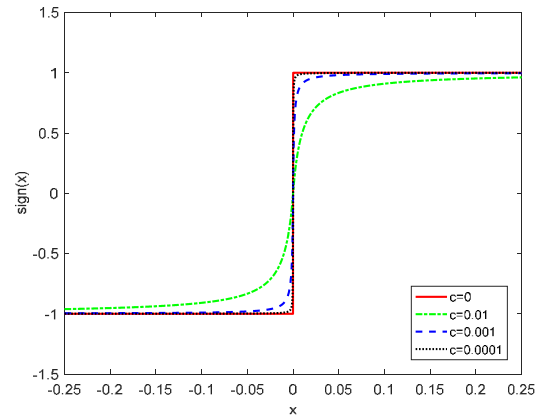
$$sign(x) = \frac{x}{|x| + c} \qquad (16)$$

Figure 3. The extent of smoothness impact by the value of c, when c=0 it represents the initial *sign* function.

where c is a positive constant. From Fig. 3 we can see that the smoothness gets better with the increasing of c. Besides, we suppose an index whose value is the error between the initial function and smoothed function when x=0.05. Similar to some project indexes, the index here is expected to less than 5%. We can calculate the indexes are 16%, 2% and 0.2% separately for c=0.01, 0.001, 0.0001. Thus, c=0.001 and c=0.0001 are both meet the index requirement. To obtain better smoothness, we choose c=0.001.

SDC is described in (15), there are just two gains in u_s and the angular velocity ω can be directly measured by a gyroscope, so SDC is a simple control approach for easy design and convenient realization. Note that the control law u_s is just used to stabilize the attitude system, when the attitude system requires outputting expected angles the control law needs to be adjusted as follows.

Suppose the errors between the expected values and actual values of *Pitch*, *Roll*, and *Yaw* are e_x, e_y, and e_z. The control law is adjusted to meet the requirement of outputting expected angles as (17).

$$u = k \begin{bmatrix} e_x \\ e_y \\ e_z \end{bmatrix} - z_1 \begin{bmatrix} \omega_x^2 sign(\omega_x) \\ \omega_y^2 sign(\omega_y) \\ \omega_z^2 sign(\omega_z) \end{bmatrix} - z_2 \begin{bmatrix} sign(\omega_x) \\ sign(\omega_y) \\ sign(\omega_z) \end{bmatrix} \qquad (17)$$

The derivative of the Nonlinear equation is complex and which makes the stability analysis too hard to be carried.

From equation (3), it is clear that $\omega \times J\omega$ donates the main nonlinearity of attitude dynamics. We can modify equation (17) as (18) so that the strict stability analysis can be done in the following.

$$u = k \begin{bmatrix} e_x \\ e_y \\ e_z \end{bmatrix} - z_1 \begin{bmatrix} \omega_x^2 sign(\omega_x) \\ \omega_y^2 sign(\omega_y) \\ \omega_z^2 sign(\omega_z) \end{bmatrix} - z_2 \begin{bmatrix} sign(\omega_x) \\ sign(\omega_y) \\ sign(\omega_z) \end{bmatrix} + \omega \times J\omega \quad (18)$$

C. Stabilization Analyze

The gains z_1 and z_2 determine the stabilization of the attitude system described in (9). Classical control theory is not applicable because this is a multi-input multi-output non-linear system. If using the Lyapunov method directly, how to choose the Lyapunov function is unknown. *Krasovskii Theorem* is convenient to analyze this non-linear system.

Lemma 1. *Krasovskii Theorem*

For the follow system

$$\dot{x} = f(x), t \geq 0$$

Define

$$F(x) = \frac{\partial f(x)}{\partial x^T} = \begin{bmatrix} \dfrac{\partial f_1(x)}{\partial x_1} & L & \dfrac{\partial f_1(x)}{\partial x_n} \\ M & & M \\ \dfrac{\partial f_n(x)}{\partial x_1} & L & \dfrac{\partial f_n(x)}{\partial x_n} \end{bmatrix} \quad (19)$$

For a non-linear continuous time-invariant system and an area around the original point $\Omega \in \Re^n$, the original point is the only equilibrium point in Ω, and $F(x) + F^T(x) < 0$ (negative definite), then the system equilibrium state $x=0$ is asymptotic stability in Ω.

Lemma 2. Suppose matrix A is a Hermite matrix and λ represents an arbitrary eigenvalue of A, then $\lambda \in \Re$, and "A is a positive definite matrix" is equivalent to "$\lambda \in \Re^+$".

Lemma 3. Suppose matrix $A = (a_{ij}) \in \Re^{n \times n}$.

If $|a_{ii}| > \sum\limits_{\substack{j=1 \\ j \neq i}}^{n} |a_{ij}| \quad (i = 1, L, n)$, call A is a strictly raw diagonal dominance matrix. If A is a strictly raw diagonal dominance matrix and all the diagonal terms are positive real numbers, then $\lambda \in \Re^+$.

From Fig. 3 we can see that the derivative of the *sign* function is symmetrical about axis y. It is valid to suppose $x>0$ when calculating the derivative of the *sign* as the postamble just uses the absolute value of the derivative. Thus, the derivative of this function as

$$\delta(x) = \left[sign(x)\right]' = \frac{c}{\left(c + |x|\right)^2} \quad (20)$$

Define

$$m_x = -2z_1 \omega_x sign(\omega_x) - z_1 \omega_x^2 \delta(\omega_x) - z_2 \delta(\omega_x)$$
$$m_y = -2z_1 \omega_y sign(\omega_y) - z_1 \omega_y^2 \delta(\omega_y) - z_2 \delta(\omega_y) \quad (21)$$
$$m_z = -2z_1 \omega_z sign(\omega_z) - z_1 \omega_z^2 \delta(\omega_z) - z_2 \delta(\omega_z)$$

According to (9), (10), and (18)

$$F = \begin{bmatrix} F_{11} & F_{12} & F_{13} \\ F_{21} & F_{22} & F_{23} \\ F_{31} & F_{32} & F_{33} \end{bmatrix} \quad (22)$$

where

$$\begin{cases} F_{11} = \dfrac{1}{J_x} m_x, F_{12} = \dfrac{J_{xy}}{J_x J_y} m_y, F_{13} = \dfrac{J_{xz}}{J_x J_z} m_z \\ F_{21} = \dfrac{J_{xy}}{J_x J_y} m_x, F_{22} = \dfrac{1}{J_y} m_y, F_{23} = \dfrac{J_{yz}}{J_y J_z} m_z \\ F_{31} = \dfrac{J_{xz}}{J_x J_z} m_x, F_{32} = \dfrac{J_{yz}}{J_y J_z} m_y, F_{33} = \dfrac{1}{J_z} m_z \end{cases} \quad (23)$$

Define $W = F^T(x) + F(x)$

$$W = \begin{bmatrix} W_{11} & W_{12} & W_{13} \\ W_{21} & W_{22} & W_{23} \\ W_{31} & W_{32} & W_{33} \end{bmatrix} \quad (24)$$

where

$$\begin{cases} W_{11} = \dfrac{2}{J_x} m_x, W_{12} = \dfrac{J_{xy}}{J_x J_y}(m_x + m_y), W_{13} = \dfrac{J_{xz}}{J_x J_z}(m_x + m_z) \\ W_{21} = \dfrac{J_{xy}}{J_x J_y}(m_x + m_y), W_{22} = \dfrac{2}{J_y} m_y, W_{23} = \dfrac{J_{yz}}{J_y J_z}(m_y + m_z) \\ W_{31} = \dfrac{J_{xz}}{J_x J_z}(m_x + m_z), W_{32} = \dfrac{J_{yz}}{J_y J_z}(m_y + m_z), W_{33} = \dfrac{2}{J_z} m_z \end{cases} \quad (25)$$

For the closed-loop system combined by (9) and (18), it is assumed that $x=0$ is the only equilibrium point in Ω.

Theorem 1. For the system combined by (9) and (18), if the matrix $-W$ satisfies the two follow conditions, then the system is asymptotic stable in Ω.

(a) All the diagonal terms of $-W$ are positive real numbers.

(b) The matrix $-W$ is a strictly raw diagonal dominance matrix.

The proof is as follow. λ_1 an arbitrary represents the eigenvalue of $-W$. From (25) we can observe that $(-W)^T = -W$, then $-W$ is a Hermite matrix. According to condition (a), (b) and *Lemma* 3, $\lambda_1 > 0$. Follow *Lemma* 2, the matrix $-W$ is a positive definite matrix, so W is a negative definite matrix. Since $x=0$ is the only equilibrium point in Ω and $F(x) + F^T(x) < 0$, according to *Lemma* 1, the system combined by (9) and (18) is asymptotic stable in Ω.

Note that Ω is the state-space area determined by the real RUAV flight requirement. Once the area Ω is defined, we can choose the control parameters z_1 and z_2 according to condition (a) and (b). From equation (21), the value of m is obviously negative, thus condition (a) is satisfied. In section II, it is noted that the off-diagonal terms of inertia matrix J can be taken as small numbers. Hence, condition (b) can be satisfied by adjusting z_1 and z_2.

There will be an example in section IV. We can know that it will cost a lot of time to calculate z_1 and z_2 by theory. Although *Theorem* 1 can guarantee the stabilization of the RUAV attitude system, it cannot guarantee to output expected angles. Therefore, in the real application, it is

inadvisable to spend much effort to calculate z_1 and z_2 to obtain an accurate range. The purpose of stabilization analysis by theory is to indicate the direction for choosing z_1 and z_2 so that the majorization of gains is simplified, in section IV will show the details.

IV. SIMULATION AND RESULTS

The simulation is implemented in C++ on VS2017. Compared with the typical simulation tool MATLAB, there are two advantages

1) The designer can modify the RUAV system with more freedom and understand the RUAV control more deeply.
2) The simulation C++ code can be easily ported to embedded processors.

However, there are some barriers that stand in the way. For example, the derivative equations have to be solved in practical approaches. The attitude calculation is a key point and it is difficult, but many articles have proposed numerous practical methods [26]. In this paper, we will just introduce how to simulate a linear time-varying system.

A. Simulation of a Linear Time-Varying System

In the following system, system matrix A is a time-varying matrix. In the process of simulation, the calculation is a discrete-time domain. In one-circle calculation, A can be seen as constant so that the calculation can follow a time-invariant system.

$$\dot{x} = Ax + Bu$$

According to linear system theory, the solution of the system is

$$x(t) = e^{A(t-t_0)}x(t_0) + \int_{t_0}^{t} e^{A(t-\tau)}B(\tau)u(\tau)d\tau \quad (26)$$

Rewrite (26) into discrete time form, with the consideration of t can only be an integral multiple of T whose typical value is 0.01s in RUAV control.

$$x(k+1) = e^{AT}x(k) + Te^{AT}Bu(k) \quad (27)$$

As the sample time T is very small, the terms of AT are also small numbers. In this paper, it is accurate enough to expand e^{AT} into the second-order Taylor series.

$$e^{AT} = I + AT + \frac{A^2T^2}{2} \quad (28)$$

Using (27) and (28), one-circle calculation can be achieved. After one-circle calculation, refreshing the system matrix A, and then go into the next circle.

B. Simulation Parameters

The following simulation parameters are obtained from an actual RUAV in our lab. The length and width are both about 0.45m. The mass is about m=1.373kg, the inertial matrix terms are

$$J_x = 0.10125\text{kg}\cdot\text{m}^2 \quad J_y = 0.10203\text{kg}\cdot\text{m}^2 \quad J_z = 0.14374\text{kg}\cdot\text{m}^2$$

$$J_{xy} = 0.00217\text{kg}\cdot\text{m}^2 \quad J_{yz} = 0.00153\text{kg}\cdot\text{m}^2 \quad J_{zx} = 0.00030\text{kg}\cdot\text{m}^2$$

According to *Theorem* 1 choose the control parameters z_1, z_2 to stabilize the system described in (9). As J_z is the biggest element in J, the condition "$-W_{33}$ is strictly raw

diagonal dominance" will play a decisive role in z_1 and z_2 selection. For conservative estimation, the amplitude of angular velocity is supposed to be A_1=15 rad/s.

If (29) is satisfied, the closed-loop system described by (9) and (18) is asymptotic stable.

$$|m_z| > \frac{J_y J_{xz}|m_x| + J_x J_{yz}|m_y|}{2J_x J_y - J_y J_{xz} - J_x J_{yz}} \quad (29)$$

$$|m_z| = 2z_1\omega_z sign(\omega_z) + z_1\omega_z^2\delta(\omega_z) + z_2\delta(\omega_z) \quad (30)$$

When $\omega_z \geq 1$rad/s, the last term of of (30) can be neglected

$$2z_1\omega_z + z_1\omega_z^2\delta(\omega_z) > \frac{J_y J_{xz} + J_x J_{yz}}{2J_x J_y - J_y J_{xz} - J_x J_{yz}}\left(2z_1 A_1 + z_1 A_1^2\right)$$

$$2z_1\omega_z + z_1\omega_z^2\delta(\omega_z) > 0.16z_1 \quad (31)$$

According to equation(31), we can estimate that z_1>0. The first two terms of (29) can be neglected when the angular velocity ω_z is small, and this treatment is conservative. When $\omega_z \leq 0.01$rad/s

$$z_2\delta(\omega_z) > \frac{J_y J_{xz} + J_x J_{yz}}{2J_x J_y - J_y J_{xz} - J_x J_{yz}}z_2 \quad (32)$$

From equation(32), We can estimate that z_2>0. When 0.01rad/s<ω_z<1 rad/s, the system is general stable. From the above analysis, stability is easy to in real applications satisfy. Generally, stability is just a basic requirement for RUAV. Hence, z_1 and z_2 need to be optimized to obtain better performance.

C. Simulations Result

The simulations are carried out for the closed-loop system combined by (9), (10), and (18). The purpose of the simulations is to show the effectiveness of SDC and gains estimation by theory. Besides, the gains are optimized by simulations. Following the estimation in section IV, we choose z_1=0.2, z_2=0.1. The value of k in (18) is unknown, we choose a group of values as k=0.1, 1, 5, 20. The system has the zero-initial condition, the expected angles as *Pitch*=1rad, *Roll*=*Yaw*=0, and simulation time is 100s, in other words, 10000 steps.

From Fig. 4(a) and (b), we can see the details of the response affected by the value of k. Fig. 4(c) shows the stabilization of the system in the whole simulation process. By this simulation, the effectiveness of the control law described by equation (18) and the gains estimation method in section IV is reliable. From Fig. 4(a), the climb speed and the overshoot are increasing as the k growing. If the value of k is too small, there will have a steady-state error. On consideration of the actual thrusts are limited, the value of k must have an upper bound. This means that we cannot increase k for higher climb speed without limitation. We expect the system can climb to 0.95 rad in 0.5s (50 steps), k≥5 meet this requirement. For the purpose to decrease the overshoot, z_1 and z_2 have to be adjusted. Firstly, adjust sensitive gain z_1, select k=5, z_2=0.1, z_1=0.2, 0.5, 0.8, 1.0, the

simulation result shows in Fig. 5. We can see that the climb speed and the overshoot decrease as the value of z_1 growing. When $z_1 > 0.5$, the climb speed cannot meet the requirement even though the overshoot is smaller. When $z_1 = 0.2$, the overshoot is about 20%, when $z_1 = 0.5$, the overshoot decreases to 7%.
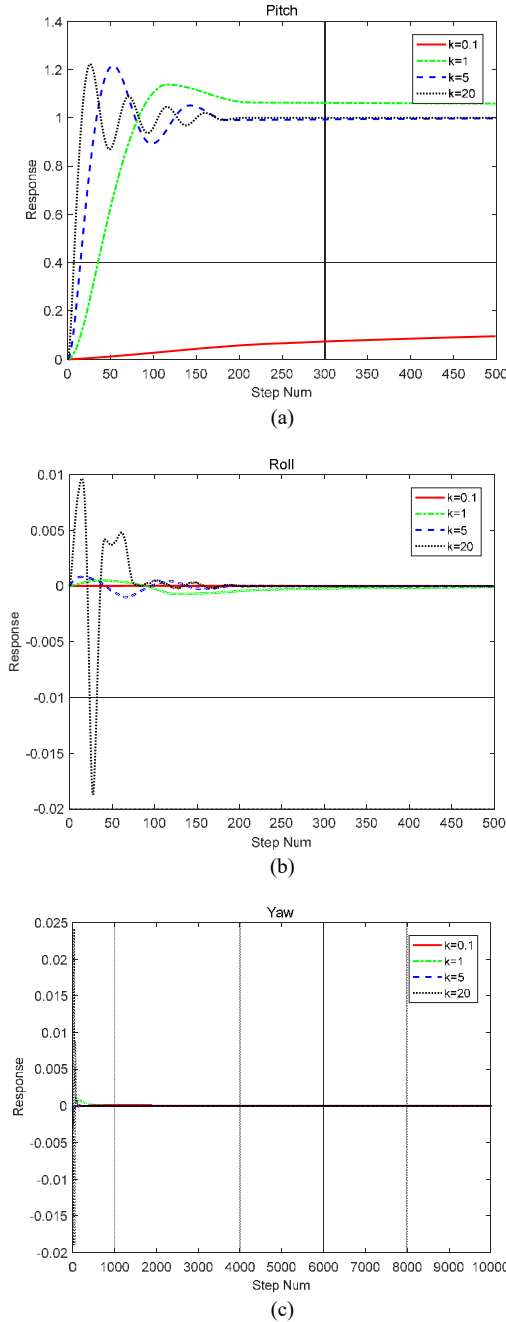

(a)

(b)

(c)

Figure 4. *Roll, Pitch, Yaw* response with different k, Inputs as *Roll*=1rad, *Pitch=Yaw*=0.

Based on the former simulations, select $k=5$, $z_1=0.5$ and $z_2=0.1$, 0.5, 1.0, 5.0. The simulation result sees in Fig. 6, the climb speed of the system decreases as the value of z_2 growing. When $k=5$, $z_1=0.5$, and $z_2=0.5$, the system has the best response performance with high climb speed and no overshoot. To show the good performance of $k=5$, $z_1=0.5$,

and $z_2=0.5$, let the system follow a square wave which is input in *Pitch* with a period of 4s (400 steps). The simulation result is shown in Fig. 7. Now let's compare the coefficient of actual air-resistance Z_1 and Z_2 with the optimal control law related gains z_1 and z_2. The values of z_1 and z_2 are much larger than Z_1 and Z_2. Therefore, the parameters of the control law do not reflect the actual air-resistance.

Let's summarize the several rules for gains adjustment.
1) The estimation in section IV of z_1 and z_2 is effective. However, it is not optimal.
2) The climb speed and overshoot will be higher as the value of k grows.
3) The system response and overshoot will be lower as the value of z_1 and z_2 grows.

In general, the rules for gains adjustment are simple, which is because the relationship between system response and gains is monotonic.
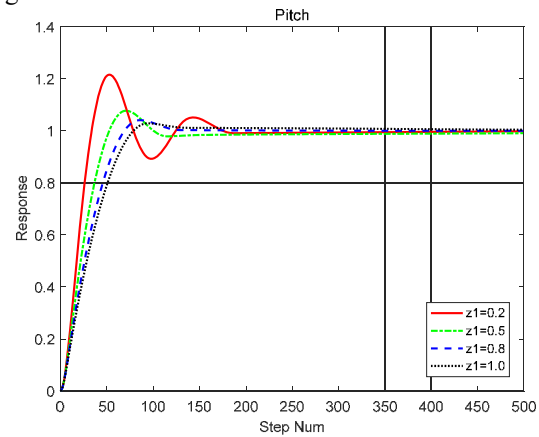

Figure 5. Adjustment of z_1 as 0.2, 0.5, 0.8, 1.0 . Inputs as *Roll*=1rad, *Pitch=Yaw*=0.
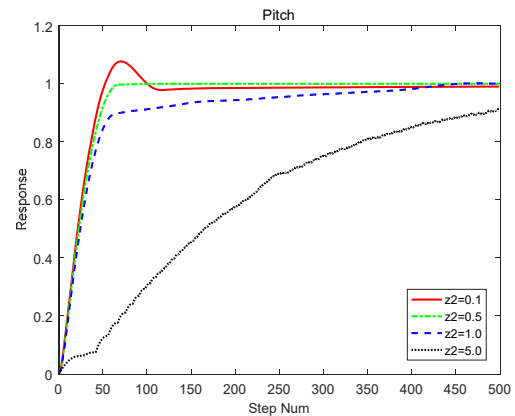

Figure 6. Adjustment of z_2 as 0.1, 0.5, 1.0, 5.0. Inputs as *Roll*=1rad, *Pitch=Yaw*=0.
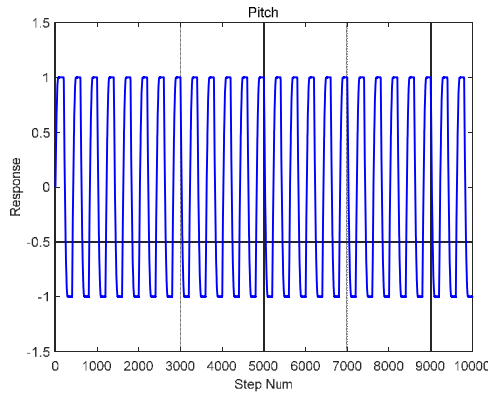
Figure 7.   Follow the square wave ith the period of 4s (400 steps) , input in *Pitch*.

The robustness test includes the ability of interference rejection and system parameters change adaption. This paper simulates two situations. The one is the RUAV disturbed by a fluctuating wind so that a suddenly angular velocity is obtained. The other is the change of the inertia matrix J, in particular, we change J_x in this paper.

The fluctuating wind make the RUAV suddenly obtain an angular velocity as
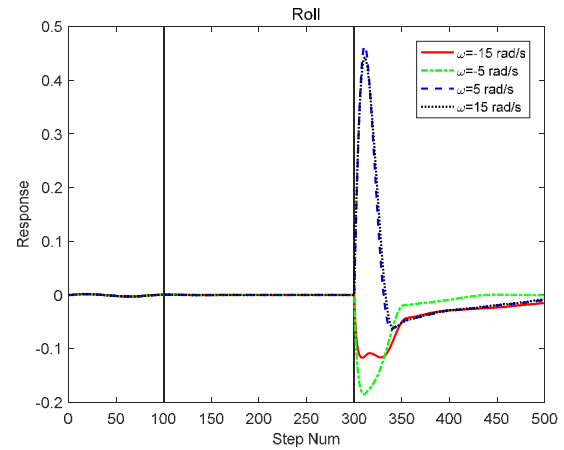
$$\omega_x = \omega_y = \omega_z = -15, \quad -5, \quad 5, \quad 15 \, \text{rad/s}$$

Firstly, a signal *Pitch*=1rad, *Roll*=*Yaw*=0 is input when t=0. When t=3s, the disturbance from wind is inserted so that the system obtains the angular velocity suddenly. The gains as k=5, z_1=0.5, and z_2=0.5. The simulation result shows in Fig.8.
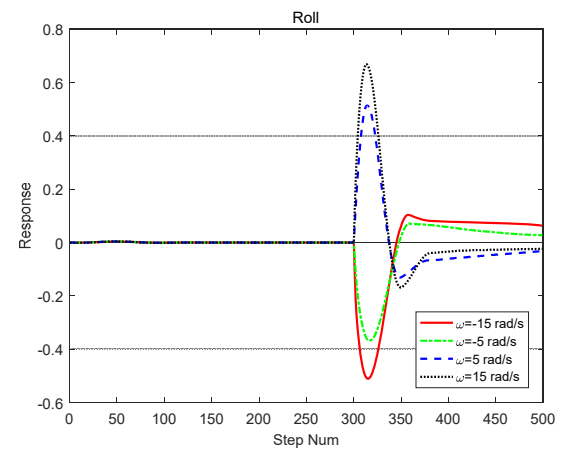
From Fig. 8, we can see the ability of interference rejection, and the closed-loop system is not sensitive to the strength of the fluctuating wind which is expressed by ω. However, there is a big movement of the angle after the disturbance, the biggest value is about 25%, it is the place that needs to be improved.
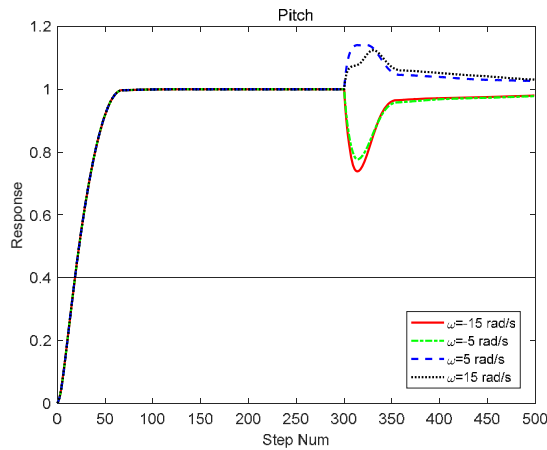
(b)

(c)

Figure 8.   Robust test for fluctuating wind with ω=-15, -5, 5, 15rad/s, and the gains as k=5, z_1=0.5, z_2=0.5.

Here we want to test the inference in section IV-B that "if z_1 over the existed upper bound, the system may lose robustness". This inference shows that the robustness will decrease as the value of z_1 growing. When t=3s, the wind disturbance is inserted with ω_x=ω_y=ω_z=15rad/s and the gains as k=5, z_1=0.5, and z_2=0.5. In this simulation, the system will lose stabilization, which is because the value of z_1 is too big. Therefore, Fig. 9 shows that the inference in section IV-B is reliable.

The inertia matrix J has a change with J_x takes the value as 0.050625, 0.10125, 0.151875, 0.2025 kg·m^2. The gains as k=5, z_1=0.5, z_2=0.5, and the input *Pitch*=1rad, *Roll*=*Yaw*=0. Fig.10 shows robustness to inertia matrix change. Simultaneously, we can see that the relationship between system response and inertia matrix change is monotonic. This means that if the system knows what is change, it is possible to accommodate the change by automatically adjust the gains.
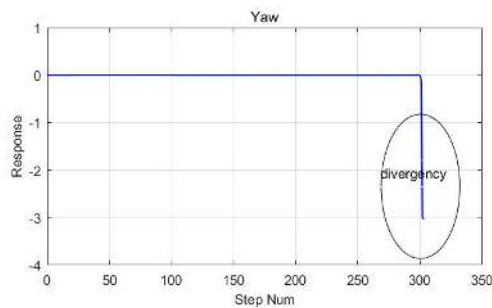
(a)

Figure 9. System loses the stabilization when fluctuating wind with ω=15 rad/s, and the gains as k=5, z_1=2, z_2=0.5.
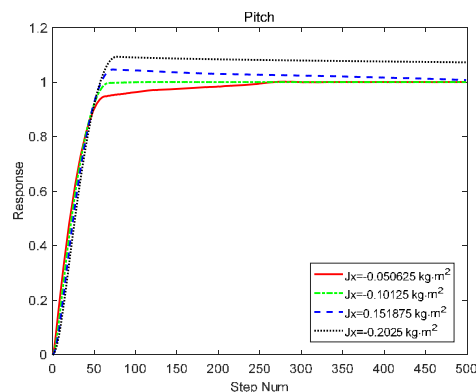

Figure 10. Jx as 0.050625, 0.10125, 0.151875, 0.2025 kg·m2 and the gains as k=5, z1=2, z2=0.5.

D. Comparison with PID

As PID is the most successful algorithm in applications, the comparison between SDC and PID is as follows. Simulated wind disturbance is shown in Fig.11 and high-frequency square-wave-disturbance with 50Hz frequency is shown in Fig.12. The gains of SDC and PID are tuned so that the response curves are almost coincident in the normal stage. From the simulation results, the response-amplitude of PID is almost 3.4 times than SDC which is caused by simulated wind disturbance, and the spike of PID is almost 5 times than SDC. However, PID is smooth than SDC when the response is small as Fig.12. No matter what, SDC is robust than PID from the simulation result.
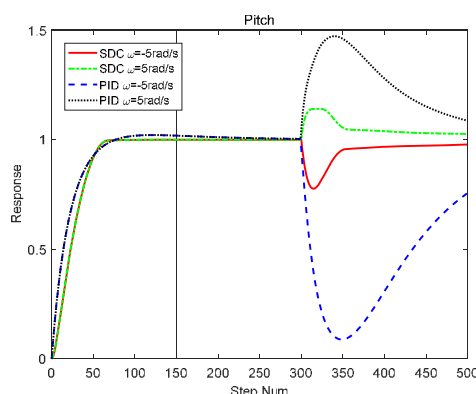

Figure 11. SDC gains as k=5, z_1=0.5, z_2=0.5; PID gains as P=0.45, I=0, D=0.05 .
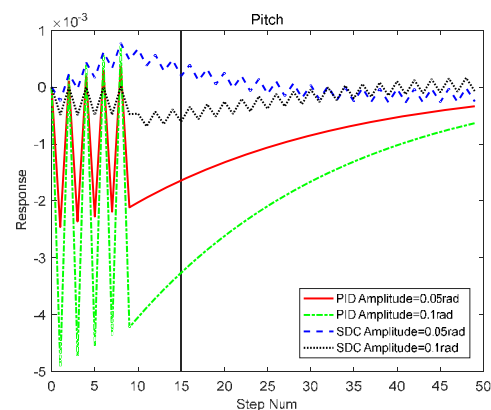

Figure 12. SDC gains as k=5, z_1=0.5, z_2=0.5; PID gains as P=0.45, I=0, D=0.05. The amplitudes of square-wave-disturbance as 0.05rad and 0.1rad at the time interval 0<t<10, and it is changed per step.

VI. CONCLUSION

In this paper, we propose a novel approach named SDC to control the attitude of RUAV. SDC is independent of model accuracy and it can be a candidate to traditional PID. Compared with SMC and MRAC, the parameters of SDC are easy to be tuned. The stabilization of the RUAV attitude system is analyzed based on *Krasovskii Theorem*, and the rules for tuning gains are given. The simulation results show the effectiveness of SDC and the estimation method for gains. After optimizing the gains, the system can climb quickly, and there is no overshoot. The simulation results also show that SDC is robust to wind disturbances and inertial parameter changes. Furthermore, the comparison with PID shows the superior robustness of SDC. In our future study, SDC is expected to control the whole RUAV system not only the attitude system. In addition, some experiments are also needed to carry out.

REFERENCES

[1] D. Giordan, Y. Hayakawa, F. Nex, F. Remondino, and P. Tarolli, "Review article: the use of remotely piloted aircraft systems (RPASs) for natural hazards monitoring and management," *Natural Hazards and Earth System Sciences,* vol. 18, no. 4, pp. 1079-1096, Apr 6 2018.

[2] S. Manfreda *et al.*, "On the Use of Unmanned Aerial Systems for Environmental Monitoring," *Remote Sensing,* vol. 10, no. 4, Apr 2018, Art. no. 641.

[3] R. Nasi *et al.*, "Estimating Biomass and Nitrogen Amount of Barley and Grass Using UAV and Aircraft Based Spectral and Photogrammetric 3D Features," *Remote Sensing,* vol. 10, no. 7, Jul 2018, Art. no. 1082.

[4] Lee H , Kim H J . Full control of control of multirotors from modelling to experiments: A survey[J]. International Journal of Control, Automation and Systems, 2017, 15(1):281-292.

[5] E. Stingu and F. L. Lewis, "A Hardware Platform for Research in Helicopter UAV Control," *Journal of Intelligent & Robotic Systems,* vol. 54, no. 1-3, pp. 387-406, Mar 2009.

[6] Wei W , Gao S , Zhong Y , et al. Random weighting estimation for systematic error of observation model in dynamic vehicle navigation[J]. International Journal of Control, Automation and Systems, 2016, 14(2):514-523.

[7] H. Efraim, S. Arogeti, A. Shapiro, and G. Weiss, "Vision Based Output Feedback Control of Micro Aerial Vehicles in Indoor

Environments," *Journal of Intelligent & Robotic Systems,* vol. 87, no. 1, pp. 169-186, Jul 2017.

[8] W. Fan, C. Xiang, and B. Xu, "Modelling, attitude controller design and flight experiments of a novel micro-ducted-fan aircraft," *Advances in Mechanical Engineering,* vol. 10, no. 3, Mar 20 2018, Art. no. 1687814018765569.

[9] Saxena S , Hote Y V . Internal model control based PID tuning using first-order filter[J]. International Journal of Control Automation & Systems, 2016, 15(1):1-11.

[10] G. Herrmann, S. K. Spurgeon, and C. Edwards, "On robust, multi-input sliding-mode based control with a state-dependent boundary layer," *Journal of Optimization Theory and Applications,* vol. 129, no. 1, pp. 89-107, Apr 2006.

[11] X. B. Xiang, C. Liu, H. S. Su, and Q. Zhang, "On decentralized adaptive full-order sliding mode control of multiple UAVs," *Isa Transactions,* vol. 71, pp. 196-205, Nov 2017.

[12] E. Ozkop, I. H. Altas, H. I. Okumus, and A. M. Sharaf, "A fuzzy logic sliding mode controlled electronic differential for a direct wheel drive EV," *International Journal of Electronics,* vol. 102, no. 11, pp. 1919-1942, Nov 2 2015.

[13] F. Ding, J. Huang, Y. Wang, J. Zhang, and S. He, "Sliding mode control with an extended disturbance observer for a class of underactuated system in cascaded form," *Nonlinear Dynamics,* vol. 90, no. 4, pp. 2571-2582, Dec 2017.

[14] M. Defoort, T. Floquet, A. Kokosy, and W. Perruquetti, "A novel higher order sliding mode control scheme," *Systems & Control Letters,* vol. 58, no. 2, pp. 102-108, Feb 2009.

[15] I. Shah and F. U. Rehman, "Smooth Higher-Order Sliding Mode Control of a Class of Underactuated Mechanical Systems," *Arabian Journal for Science and Engineering,* vol. 42, no. 12, pp. 5147-5164, Dec 2017.

[16] G. Perozzi, D. Efimov, J. M. Biannic, and L. Planckaert, "Trajectory tracking for a quadrotor under wind perturbations: sliding mode control with state-dependent gains," *Journal of the Franklin Institute-Engineering and Applied Mathematics,* vol. 355, no. 12, pp. 4809-4838, Aug 2018.

[17] Saif A W A , Aliyu A , Dhaifallah M A , et al. Decentralized Backstepping Control of a Quadrotor with Tilted-rotor under Wind Gusts[J]. International Journal of Control, Automation and Systems, 2018, 16(5):2458-2472.

[18] Z. A. Ali, D. B. Wang, and M. Aamir, "Fuzzy-Based Hybrid Control Algorithm for the Stabilization of a Tri-Rotor UAV," *Sensors,* vol. 16, no. 5, May 2016, Art. no. 652.

[19] S. Zhang, Q. Fei, J. Liang, Q. Geng, and Ieee, "Modeling and Control for Longitudinal Attitude of a Twin-Rotor Tail-sitter Unmanned Aerial Vehicle," in *13th IEEE International Conference on Control & Automation (ICCA)*, Ohrid, MACEDONIA, 2017, pp. 816-821, 2017.

[20] Y. Yildiz, M. Unel, and A. E. Demirel, "Nonlinear hierarchical control of a quad tilt-wing UAV: An adaptive control approach," *International Journal of Adaptive Control and Signal Processing,* vol. 31, no. 9, pp. 1245-1264, Sep 2017.

[21] I. Sadeghzadeh, A. Mehta, and Y. Zhang, "Fault/damage tolerant control of a quadrotor helicopter UAV using model reference adaptive control and gain-scheduled PID," in *Proc. AIAA Guid., Navigat., Control Conf.,* Portland, OR, 2011, pp. 1–20.

[22] Z. T. Dydek, A. M. Annaswamy, and E. Lavretsky, "Adaptive Control of Quadrotor UAVs: A Design Trade Study With Flight Evaluations," *Ieee Transactions on Control Systems Technology,* vol. 21, no. 4, pp. 1400-1406, Jul 2013.

[23] S. Zeghlache, H. Mekki, A. Bouguerra, and A. Djerioui, "Actuator fault tolerant control using adaptive RBFNN fuzzy sliding mode controller for coaxial octorotor UAV," (in English), *ISA transactions,* 2018 Jun 06 (Epub 2018 Jun 2018.

[24] Y. Xu, W. Sun, and P. Li, "A Miniature Integrated Navigation System for Rotary-Wing Unmanned Aerial Vehicles," *International Journal of Aerospace Engineering,* 2014, Art. no. 748940.

[25] J. Dou, X. Kong, X. Chen, and B. Wen, "Output feedback observer-based dynamic surface controller for quadrotor UAV using quaternion representation," *Proceedings of the Institution of Mechanical Engineers Part G-Journal of Aerospace Engineering,* vol. 231, no. 14, pp. 2537-2548, Dec 2017.

[26] J. Dou, X. Kong, X. Chen, and B. Wen, "Output feedback observer-based dynamic surface controller for quadrotor UAV using quaternion representation," *Proceedings of the Institution of Mechanical Engineers Part G-Journal of Aerospace Engineering,* vol. 231, no. 14, pp. 2537-2548, Dec 2017.

[27] S. Bouabdallah, P. Murrieri, R. Siegwart, and Ieee, "Design and control of an indoor micro quadrotor," in *IEEE International Conference on Robotics and Automation*, New Orleans, LA, 2004, pp. 4393-4398, 2004.

[28] G. Hoffmann, H. Huang, S. Waslander, and C. Tomlin, "Quadrotor helicopter flight dynamics and control: Theory and experiment," in Proc.*AIAA Guid., Navigat., Control Conf.,* Hilton Head, SC, 2007, pp. 1–20.

[29] X.-Q. Sun, Y.-F. Cai, C.-C. Yuan, S.-H. Wang, and L. Chen, "Fuzzy Sliding Mode Control for the Vehicle Height and Leveling Adjustment System of an Electronic Air Suspension," *Chinese Journal of Mechanical Engineering,* vol. 31, no. 1, Dec 2018, Art. no. Unsp 25.

[30] F. Golnary and H. Moradi, "Design and comparison of quasi continuous sliding mode control with feedback linearization for a large scale wind turbine with wind speed estimation," *Renewable Energy,* vol. 127, pp. 495-508, Nov 2018.

[31] H.Alwi, C.Edwards and C.- P. Tan, *Fault Detection and Fault tolerant Control Using Sliding Modes.* National Defense Industry Press, Beijing, ISBN 978-7-118-09546-3,2014.

[32] A. Odry, R. Fuller, I. J. Rudas, and P. Odry, "Kalman filter for mobile-robot attitude estimation: Novel optimized and adaptive solutions," *Mechanical Systems and Signal Processing,* vol. 110, pp. 569-589, Sep 15 2018.

[33] Yun S , Lee Y J , Sung S . Range/optical flow-aided integrated navigation system in a strapdown sensor configuration[J]. International Journal of Control Automation & Systems, 2016, 14(1):229-241.

[34] Xi C, Dong J. Adaptive asymptotic tracking control of uncertain nonlinear time-delay systems depended on delay estimation information[J]. Applied Mathematics and Computation, 391: 125662.

[35] Xi C, Dong J. Adaptive exact sliding tracking control of high‐order strict‐feedback systems with mismatched nonlinearities and external disturbances[J]. International Journal of Robust and Nonlinear Control, 2020.

[36] Sun Y, Xu J, Qiang H and Lin G. Adaptive neural-fuzzy robust position control scheme for maglev train systems with experimental verification [J]. IEEE Transactions on Industrial Electronics, 2019, 66(11): 8589-8599

[37] Sun Y, Qiang H, Xu J, et al. Internet of Things-based online condition monitor and improved adaptive fuzzy control for a medium-low-speed maglev train system[J]. IEEE Transactions on Industrial Informatics, 2020, 16(4): 2629-2639

[38] C. Li, Y. Zhang, and P. Li, "Full control of a quadrotor using parameter-scheduled backstepping method: implementation and experimental tests," *Nonlinear Dynamics,* vol. 89, no. 2, pp. 1259-1278, Jul 2017.

[39] Y. Yu, S. Yang, M. Wang, C. Li, Z. Li, and Ieee, "High Performance Full Attitude Control of a Quadrotor on SO(3)," in *IEEE International Conference on Robotics and Automation (ICRA)*, Seattle, WA, 2015.

[40] Lee H , Kim H J . Trajectory tracking control of multirotors from modelling to experiments: A survey[J]. International Journal of Control, Automation and Systems, 2017, 15(1):281-292.

Run Ye received the B.S. degree in automation from Anhui University, Hefei, China, in 2010 and the M.S. degree in control engineering from University of Electronic Science and Technology of China, Chengdu, China, in 2013. From 2015 to 2016, he was a joint Ph.D. student in University of Ottawa, Ottawa, Canada, and received the Ph.D. degree in control science and engineering from University of Electronic Science and Technology of China, Chengdu, China, in 2013. Since 2017, he has served as a research assistant in the School of Automation Engineering,

University of Electronic Science and Technology of China, Chengdu, China. His research interests include unmanned system, intelligent control, intelligent information processing, neural networks and wireless communication and networks.

Peng Liu received the B.S., degree in Civil Engineering from Central South University of China in 2017. He is now working toward the M.S. degree with the School of Automation Engineering, University of Electronic Science and Technology of China, Chengdu, China. His research interests includes Control and Navigation Algorithms of UAV, Time Series Prediction and Mechanical Analysis of Structures.

Kaibo Shi received Ph.D. degree in School of Automation Engineering at the University of Electronic Science and Technology of China. He is a professor of School of Information Sciences and Engineering, Chengdu University. From September 2014 to September 2015, he was a visiting scholar at the Department of Applied Mathematics, University of Waterloo, Waterloo, Ontario, Canada. He was Research Assistant with the Department of Computer and Information Science,Faculty of Science and Technology, University of Macau, Taipa, from May 2016 to Jun 2016 and January 2017 to October 2017. He was also a Visiting Scholar with the Department of Electrical Engineering, Yeungnam University, Gyeongsan, South Korea, from December 2019 to January 2020. His current research interests include stability theorem, robust control, sampled-data control systems, networked control systems, Lurie chaotic systems, stochastic systems and neural networks. He is the author or coauthor of over 60 research articles. He is a very active reviewer for many international journals.

Bin Yan is a lecturer at the University of Electronic Science and Technology of China, Chengdu, China. In 2009 he received his Ph.D. from the University of Electronic Science and Technology of China, Chengdu, China. His research interests include unmanned system, intelligent control, intelligent information processing, wireless communication and network and machine vision.